IOP Conference Series: Earth and Environmental Science

PAPER • OPEN ACCESS

Research on Hydraulic Speed Control System of Ship Crane Anti-Rolling Device

To cite this article: Yang Ji *et al* 2019 *IOP Conf. Ser.: Earth Environ. Sci.* **295** 042130

IOP Conf. Series: Earth and Environmental Science **295** (2019) 042130 doi:10.1088/1755-1315/295/4/042130

Research on Hydraulic Speed Control System of Ship Crane Anti-Rolling Device

Yang Ji, Hu Wang, Haiquan Chen[*] and Mingxuan Guo

College of Marine Engineering, Dalian Maritime University, Dalian, Liaoning, 116026, China

[*]Haiquan Chen's e-mail: chenapec@dlmu.edu.cn

Abstract. Ship cranes will be shaken sharply due to the influence of additional loads such as wind, waves and current during operation. Due to the influence of additional loads such as wind, waves and flow, the marine crane in operation will cause the cargo to shake sharply, which reduces the efficiency of the work greatly. In order to solve this problem, a three-rope traction type anti-rolling device is designed. In this paper, a hydraulic speed control system of the crane anti-rolling device is designed， the boundary conditions of the traction cable load are analysed, The boundary conditions of the traction cable load are analyzed, and the parameter matching of the main components such as hydraulic motor and hydraulic pump in the speed control system is studied.

1. Introduction

Marine cranes are mainly used for military ship replenishment, ship port loading and unloading operations, and the placement and recovery of marine buoy structures. They are one of the core technical equipment in the field of ship and ocean engineering. However, due to the typical under actuated system of the crane structure and the complex and ever-changing environment at sea, it is inevitable that the ship crane will have a large swing during operation. It is especially necessary to study the ship crane anti-rolling device. Ngo et al. [1] proposed a side swing control mechanism for container crane anti-rolling, which simplified the swing of the load and the movement of the trolley into one picture, and used the empirical control law to perform the anti-rolling. The simulation confirmed that the structure has better anti-rolling. performance. JANG et al. [2] established a dynamic model of a marine container crane and used the T-S fuzzy control method to control the swing of the crane. Han Guangdong et al [3] designed a ship crane lifting plate anti-rolling device, established the hoisting kinematics equation with or without the hanging plate and built a test bench to verify the effectiveness of the anti-rolling device. Parker and Graziano et al. [4] proposed the use of RBTS (Rider Block Tagline System) for active control of the swinging of marine cranes. The proposed method saves 80% of energy when the same anti-rolling effect is achieved compared to the electronic anti-swing method. Further, Ku and Cha et al. [5] used the PD controller to realize the tension control of the RBTS traction cable, and carried out the experiment using the 1:100 marine crane scale model. The experiment proved that the hoisting swing was effectively suppressed.

This paper introduces a three-rope traction marine anti-rolling crane, designs the hydraulic system of the anti-rolling device of the crane, focuses on the analysis of the speed control scheme of the hydraulic system, and provides a reference for the design and component selection of hydraulic speed control loops for engineering machinery under complex conditions.

IOP Conf. Series: Earth and Environmental Science **295** (2019) 042130 doi:10.1088/1755-1315/295/4/042130

2. Basic working principle of the anti-rolling device

The three-rope traction type marine anti-rolling crane is composed of a crane body, a main boom, a folding arm, a hanging plate and a hook. In addition to the lifting, swinging and luffing mechanism of the crane itself, it is also equipped with a three-rope traction mechanical anti-rolling device. Figure 1 shows the overall structure of the ship's anti-rolling crane. One end of the left and right traction cables is wound on two separate reels. The other end of the pulley block that bypasses the symmetrical arrangement of the top of the folding arm is connected to the hook on the hanging plate. The front traction cable is connected to the reel at one end of the pulley block of the front end of the main boom, and the other end is fixed to the hook at the front of the suspension plate. Three anti-rolling motors are connected to the three reels by their respective reducers， they are arranged together inside the crane base and connected to the external valve member, and the control system and the hydraulic station are connected by hydraulic lines. The three traction cables are tensioned by the hydraulic system and form a stable triangular structure in the space, which can suppress the swing of the cargo in any direction, thereby achieving the purpose of reducing the swing of the hanging object.

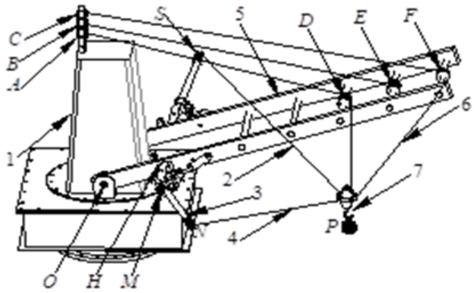

Figure 1. Crane equipped with mechanical anti-swing device

3. Design of Hydraulic system

The ship crane is affected by the movement of the ship's pedestal during the operation. The hoisting will result in rapid and irregular swinging due to the ship's roll, pitch, heave motion and its own inertia. Therefore, the hydraulic system of the anti-rolling device must have a speed control function and a certain impact resistance.

In a hydraulic system, the speed of the actuator is controlled by the flow supplied to the actuator, so the control of the flow is essentially the control of the speed of the actuator. The hydraulic speed control system is divided into a valve-controlled hydraulic system and a pump-controlled hydraulic system according to the control mode. The hydraulic system with pump-controlled volumetric speed regulation is nonlinear and the control effect is not satisfactory. Therefore, the speed control design of the anti-rolling device of the marine anti-rolling crane only considers the valve-controlled hydraulic speed control system.

The speed regulation function of the hydraulic system is usually realized by adding a throttle valve in the speed regulation loop of the hydraulic system, and the flow rate of the actuator is changed by adjusting the area of the throttle valve port to achieve the purpose of speed regulation. Ignore the leakage factor, according to the principle of flow continuity, the flow through the actuator is the flow through the orifice.

$$q = C_d A \sqrt{\frac{2}{\rho}} \Delta p^{\frac{1}{2}} \tag{1}$$

In the formula: q is the flow rate through the orifice, Cd is the throttle port flow coefficient, A is the flow area of the throttle port, and ρ is the density of the hydraulic oil, Δp is the pressure difference before and after the throttle valve.

According to the analysis of formula 1, the flow coefficient can be regarded as a constant. When the valve opening of the throttle valve is constant, the flow rate into the actuator is affected by the differential pressure between the inlet and outlet of the throttle valve. When the actuator load changes, the differential pressure between the inlet and outlet of the throttle valve changes, resulting in unstable actuator speed. In front of the throttle valve, a certain differential pressure reducing valve is connected in series to form a proportional speed regulating valve. The pressure difference between the inlet and outlet of the throttle valve is basically stabilized by the pressure compensation function of the differential pressure reducing valve, and the influence of the load change on the speed is minimized. The structural principle of the proportional speed control valve is shown in Figure 2.

The inlet pressure of the differential pressure reducing valve is p1, the outlet pressure is p2, and the outlet pressure of the throttle valve is p3. The proportional speed control valve flow is determined by the pressure difference across the throttle valve (p2-p3). P2 and p3 act as pressure feedback signals to the two ends of the pressure reducing valve spool respectively, and cooperate with the pressure of the pressure reducing valve spring to balance the pressure reducing valve spool. When the load becomes larger, the valve body of the pressure reducing valve moves to the right, the opening degree of the pressure reducing valve port becomes larger, the pressure reducing effect is weakened, and the outlet pressure p2 of the pressure reducing valve becomes larger. Further, the pressure difference (p2-p3) at both ends of the throttle valve is substantially unchanged, which reduces the effect of load changes on the proportional speed control valve flow.

Figure 3 is a schematic diagram of the hydraulic system of the anti-rolling device, which mainly drives the quantitative motor of each branch by the quantitative pump, and adjusts the rotation speed of the anti-rolling motor under different working conditions by using the proportional speed regulating valve. The PLC controller receives the signal of the tension sensor and controls the spool action of the electromagnetic reversing valve after analysing and processing, so as to realize the commutation of the anti-rolling hydraulic motor. The anti-rolling motor drives the anti-rolling winch to rotate forward and reverse to complete the retracting and releasing action of the traction cable, thereby realizing the anti-rolling function. The speed control loop of the hydraulic system adopts a throttle valve throttle speed control loop. Since the pressure difference between the two ends of the speed control valve is basically not affected by the load change, the flow rate only depends on the overflow area of the throttle port. It can greatly improve the speed stiffness of the speed control loop and improve the stability of the speed.

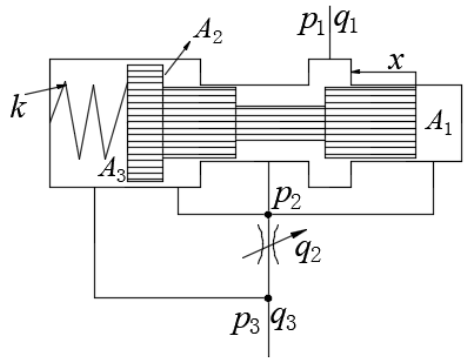

Figure 2. Speed control valve schematic

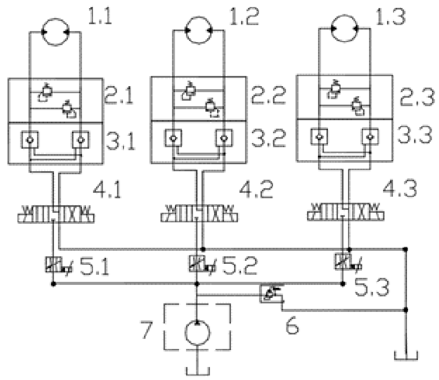

Figure 3. Anti-rolling device hydraulic system

4. Analysis of boundary conditions of traction cable load tension

The points in Figure 4 have the same meanings as the points in Figure 1.G is the weight of the hoisting weight ($G = mg$), T is the main rope tension, F1, F2 and F3 are the tension of the traction cable I, the traction cable II and the traction cable III respectively, and the angle α is the angle between the traction cable I and the positive direction of the Z axis. The angle β and the angle γ are the angles between the traction cable II and the traction cable III and the negative direction of the X-axis, respectively. The hoisting weight maintains static balance under the action of its own gravity, the main sling tension and the tension of the three traction cables. When the hoisting weight is in the state of stress balance, the PD section of the main sling is in a vertical state, and P, F, and D are in the XOZ plane, and the tension of the traction cable I in the Y direction is 0. Due to the symmetry of the space poses of the traction cables II and III, as long as the tension of the two traction cables is equal, the resultant force of the two traction cables in the Y direction is zero. Therefore, it is only necessary to consider the static balance problem of the tension in the X direction and the Z direction. The components that define the tension of the traction cables I, II, and III in the X direction are F1x, F2x, and F3x, respectively, and the three traction cable components in the Z direction are F_{1Z}, F_{2Z}, and F_{3Z}, respectively. According to the spatial geometry, the components of the three traction cables in the X direction are:

$$\begin{cases} F_{1x} = |F_1|\sin\alpha \\ F_{2x} = |F_2|\cos\beta \\ F_{3x} = |F_3|\cos\gamma \end{cases} \tag{2}$$

The components in the Z direction:

$$\begin{cases} F_{1z} = |F_1|\cos\alpha \\ F_{2z} = |F_2|\sin\beta \\ F_{3z} = |F_3|\sin\gamma \end{cases} \tag{3}$$

where, $\sin\alpha = \frac{x_F - x_P}{L_{PF}}, \cos\alpha = \frac{z_F - z_P}{L_{PF}}, \sin\beta = \frac{z_S - z_P}{L_{PS}}, \cos\beta = \frac{x_P - x_S}{L_{PS}}, \sin\gamma = \frac{z_N - z_P}{L_{PN}}, \cos\gamma = \frac{x_P - x_N}{L_{PN}}$; Due to the symmetry of N and S, $L_{PS}=L_{PN}$

The static balance equation in the X and Z directions:

$$F_{1x} - F_{2x} - F_{3x} = 0 \tag{4}$$

$$F_{1z} - F_{2z} - F_{3z} - mg + T = 0 \tag{5}$$

Due to the symmetry of the space pose of the traction cables II and III, it is easy to know the following relationship:

$$|\mathbf{F_2}| = |\mathbf{F_3}| \tag{6}$$

$$\cos\beta = \cos\gamma \tag{7}$$

$$\sin\beta = \sin\gamma \tag{8}$$

Finishing the tension relationship between the main sling tension and the sling gravity and the traction cable I:

$$T = mg + |\mathbf{F_1}|(\sin\alpha\tan\beta - \cos\alpha) \tag{9}$$

Since the sling is a flexible member, only the pulling force can be applied, and the thrust cannot be applied. Therefore, the condition that must be satisfied $T \geq 0$, that is the tension constraint of the traction cable I

$$\cos\alpha - \sin\alpha\tan\beta \leq \frac{mg}{|\mathbf{F_1}|} \tag{10}$$

Combined with the actual size of the laboratory site, the system parameters are taken as: L_{OF} =1.70m， L_{OH} =0.32m， L_{HM} =0.25m， L_{MN} =0.75m， L_{OD}=1.20m， L_{OK}=0.12m， L_{CK}=0.90m， β=10°， m=25kg, the working space of the crane is set to: l =0.2~1.4m， ϕ=0~80°。

The trend of K is simulated by MATLAB in the crane working space as shown in Figure 5， and the definition of the tension constraint coefficient of the traction cable I as K

$$K = \cos\alpha - \sin\alpha\tan\beta \leq \frac{\mathrm{mg}}{|F_1|} \tag{11}$$

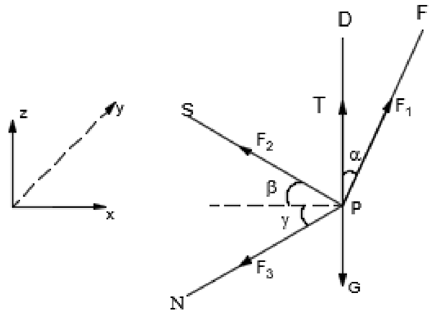

Figure 4. Traction cable anti-rolling device static analysis diagram

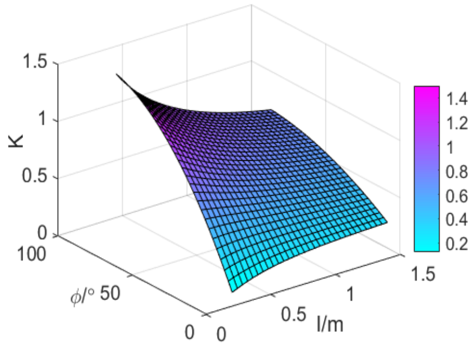

Figure 5. K's trend

It can be seen from Figure 5 that the tension constraint coefficient K of the traction cable I ranges from 0.1 to 1.5, and the value becomes significantly larger as the angle of change increases. The maximum value is obtained when the length of the main sling is 0.2m and the angle of deformation is 80°.When the length of the main sling is 0.2m and the angle of change is 0°, the minimum value is obtained. When K reaches the minimum value, F_1 takes the maximum value.

5. Selection of hydraulic components

5.1 Anti-rolling hydraulic motor selection

The maximum output torque of the hydraulic motor determines whether the hydraulic motor works normally when it withstands the maximum pulling force of the traction cable.

The ship anti-rolling crane test bench is equipped with pulley block on the rocker arm to reduce the volume of the hydraulic components, save costs and improve space utilization. According to the maximum tension value of the traction cable I in the working space of the crane, the maximum static tensile force of the anti-shake device wire rope can be obtained.

$$S = \frac{F_{1\max}}{m} \quad (12)$$

In the formula: m is the pulley group magnification

Because the load of the anti-roll test rig is small, the appropriate motor is selected to make its own torque output enough to drive the load. Therefore, the reducer is not used, and the reel is directly connected with the motor. After calculation, the diameter d of the wire rope of the anti-rolling device and the diameter D of the reel can be determined, and the maximum load torque of the anti-rolling reel can be obtained.

$$T_0 = \frac{\phi_n S(\mathrm{D}+\mathrm{d})}{2\eta_t} \quad (13)$$

In the formula: Φ_n is the system dynamic load coefficient; η_t is the mechanical efficiency of the anti-rolling drum

Then the maximum load torque output by the hydraulic motor

$$T_q = \frac{T_0}{\eta_m} \quad (14)$$

In the formula, η_m is the shaft transfer efficiency;

Since the reel and the motor are directly connected, the full load speed of the motor is equal to the reel speed, Maximum full load speed required by the motor:

$$n_0 = \frac{m v_{\max}}{\pi(\mathrm{D}+\mathrm{d})} \quad (15)$$

In the formula, A is the maximum value of the traction cable I speed, taking the maximum working speed of the main sling

The speed of the selected motor must reach the maximum full load speed and the maximum output torque must be greater than T_q .The motor has the highest working pressure when the maximum torque is output. Since the traction cable load is not large, the differential pressure of the inlet and outlet of the hydraulic motor is selected as $\Delta P = 10MPa$, and the displacement of the required hydraulic motor is calculated:

$$V_0 = \frac{2\pi T_q}{\Delta p \eta_{qm}} \tag{16}$$

In the formula: is the mechanical efficiency of the anti-rolling hydraulic motor

According to the design parameters of formulas (14)-(16) and the anti-rolling device of the marine crane, parameters such as torque, system pressure, displacement, and rotational speed are initially obtained. According to this, the selection of the anti-rolling hydraulic motor whose parameters are larger than the above parameter values

5.2 Anti-rolling hydraulic pump selection

In order to meet the normal operation of the anti-rolling hydraulic motor under various working conditions, the maximum pressure of the anti-rolling hydraulic pump must be able to overcome the load pressure and the pressure loss of the hydraulic system to drive the hydraulic motor to work. Then it can be determined that the working pressure of the hydraulic pump is

$$P_1 \geq P_0 + \sum P \tag{17}$$

In the formula: P_0 is the maximum working pressure of the anti-rolling hydraulic motor; $\sum P$ is the sum of the pressure loss and the local loss along the path.

The displacement of the hydraulic pump determines the amount of fuel supplied to the motor, which in turn determines whether the motor can meet the requirements under various complicated conditions. Therefore, the flow rate of the anti-rolling hydraulic pump must meet the maximum flow required for the anti-rolling motor:

$$q_0 = \frac{V_0 n_0 \times 10^{-3}}{\eta_{mv} \eta_v} \tag{18}$$

In the formula: η_{mv} is the hydraulic motor volumetric efficiency; η_v is the volumetric efficiency of the liquid motor inlet line.

Hydraulic pump flow

$$Q = Kq_0 \tag{19}$$

In the formula: K is the system leakage coefficient;

It can be known from the formulas (17)-(19) that the displacement and the working pressure of the hydraulic pump ， according to this reference, the hydraulic pump can be selected to meet the corresponding technical parameter model.

6. Conclusion

It mainly designs the hydraulic speed control system of a marine crane anti-rolling device and analyses the characteristics of several throttling speed control modes, select the throttling speed control circuit with speed control valve, and maintain the pressure difference between the inlet and outlet of the throttle valve basically stabilized by the pressure compensation function of the differential pressure reducing valve. This improves the speed rigidity of the speed control loop and improves the stability of the speed.

Based on the actual design of the marine anti-rolling crane, a mathematical model is established to analyse the main parameters of the hydraulic motor and hydraulic pump in the hydraulic system under the design conditions. According to the theoretical calculations and related engineering machinery samples, hydraulic equipment can be selected according to the design conditions.

IOP Conf. Series: Earth and Environmental Science **295** (2019) 042130 doi:10.1088/1755-1315/295/4/042130

References

[1] Ngo Q H, Hong K. Sliding-Mode Antisway Control of an Offshore Container Crane[J]. IEEE/ASME Transactions on Mechatronics, 2012, 17(2):201-209.

[2] Jang J H, Kwon S H, Jeung E T. Pendulation reduction on ship-mounted container crane via T-S fuzzy model[J]. Journal of Central South University of Technology, 2012, 19(1):163-167.

[3] Han Guangdong, Zhang Tong, Chen Haiquan, et al. Modeling and testing of anti-rolling device for the marine crane. Science Technology and Engineering, 2017， 17(23):305-310.

[4] Gordon Parker, Michael Graziano, Frank Leban, et al. Reducing crane payload swing using a rider block tagline control system[C]// OCEANS 2007. Europe. Aberdeen, Scotland, 2007:1-5.

[5] Nam-Kug Ku, Ju-Hwan Cha, Myung-Il Roh, et al. A tagline proportional–derivative control method for the anti-swing motion of a heavy load suspended by a floating crane in waves[J]. Proceedings of the Institution of Mechanical Engineers, Part M: Journal of Engineering for the Maritime Environment, 2013, 227(4): 357-366.